NIH Public Access
Author Manuscript
Magn Reson Imaging. Author manuscript; available in PMC 2013 February 1.

Published in final edited form as:
Magn Reson Imaging. 2012 February ; 30(2): 271–282. doi:10.1016/j.mri.2011.09.025.

Imaging longitudinal changes in articular cartilage and bone following doxycycline treatment in a rabbit anterior cruciate ligament transection model of osteoarthritis,,,☆,☆☆,★,★★

James R. Pinney[a,*], **Carmen Taylor**[b], **Ryan Doan**[b], **Andrew J. Burghardt**[b], **Xiaojuan Li**[a,b,c], **Hubert T. Kim**[c], **C. Benjamin Ma**[c], and **Sharmila Majumdar**[a,b,c]

[a]UC Berkeley-UCSF Graduate Program in Bioengineering, San Francisco, CA 94158-2330, USA

[b]Department of Radiology and Biomedical Imaging, University of California, San Francisco, San Francisco, CA 94143-0628, USA

[c]Department of Orthopaedic Surgery, University of California, San Francisco, San Francisco, CA 94143, USA

Abstract

Objective—The development of osteoarthritis following traumatic anterior cruciate ligament (ACL) injury is well established. However, few reliable indicators of early osteoarthritic changes have been established, which has limited the development of effective therapies. $T_{1\rho}$ and T_2 mapping techniques have the ability to provide highly accurate and quantitative measurements of articular cartilage degeneration in vivo. Relating these cartilaginous changes to high-resolution bone-densitometric evaluations of the late-stage osteoarthritic bone is crucial in elucidating the mechanisms of development of traumatic osteoarthritis (OA) and potential therapies for early- or late-stage intervention.

Methods—Twelve rabbits were monitored with in vivo magnetic resonance imaging (MRI) scans following ACL transection surgery with a contralateral leg sham operation. Six of the rabbits were treated with oral doxycycline for the duration of the experiment. At 12 weeks, the excised knees from three animals from each group (*n*=6 overall) were subjected to micro-computed tomography (CT) analysis.

Results—Consistent with previous studies, initial elevations in $T_{1\rho}$ and T_2 values in ACL-transected animals were observed with relative normalization towards values see in sham-operated

☆Contributions: James Pinney contributed to assembly, analysis and interpretation of the data and was responsible for drafting the article. Carmen Taylor and Ryan Doan contributed to the study design and data collection as well as drafting and revision of the article. Andrew Burghardt provided technical support in data collection and analysis as well as critical revision of the final manuscript for intellectual content. Xiaojuan Li critically reviewed the article in addition to providing concept design. Drs. Hubert T. Kim and Benjamin Ma provided assistance and technical knowledge for developing the appropriate animal model, experiment design and data collection and critically reviewed the article for content. Sharmila Majumdar contributed to the conception and design of the study, data analysis plans and logistical support to all research, as well as critical review of the article. Funding was obtained by Drs. Ma and Majumdar. All parties have reviewed and approved the final version of the article for submission.

☆☆Role of funding: This work was supported by grant A108301 from the American Orthopedics Society for Sports Medicine and National Institutes of Health R01 AG17762. This study is being supported by AOSSM Cartilage Initiative Grant (C.B.M.). The study sponsor had no involvement in study design, data collection, analysis, interpretation or manuscript production.

★Conflict of interest statement: There are no conflicts of interest to report for any of the authors of this manuscript.

★★Animal studies: All animal experiments were carried out using Good Laboratory Practices and were in accordance with institutional review and guidelines.

© 2011 Elsevier Inc. All rights reserved.

*Corresponding author. MSTP, UC Berkeley-UCSF Graduate Program in Bioengineering, Mission Bay, UCSF, San Francisco, CA 94158-2330, USA. Tel.: +1 415 514 9695. james.pinney@gmail.com, james.pinney@ucsf.edu (J.R. Pinney).

NIH-PA Author Manuscript
NIH-PA Author Manuscript
NIH-PA Author Manuscript

NIH-PA Author Manuscript

NIH-PA Author Manuscript

NIH-PA Author Manuscript

legs over the 12-week study. This biphasic pattern could hold diagnostic potential to differentiate osteoarthritic cartilage by tracking the relative proportions of $T_{1\rho}$ and T_2 values as they rise with inflammation then fall as collagen and proteoglycan loss leads to further dehydration. The addition of doxycycline resulted in inconclusive, yet potentially interesting, cartilaginous changes in several compartments of the rabbit legs. Micro-CT studies demonstrated decreased bone densitometrics in ACL-transected knees. Correlation studies suggest that the cartilaginous changes may be associated with some aspects of bony change and the development of OA.

Conclusion—We conclude that there are definite relationships between cartilaginous changes as seen on MRI and late-stage microstructural bony changes after traumatic ACL injury in rabbits. In addition, doxycycline may show promise in mitigating early-stage cartilage damage that may serve to lessen late-stage osteoarthritic changes. This study demonstrates the ability to track OA progression and therapeutic efficacy with imaging modalities in vivo.

Keywords

Osteoarthritis; T(1rho); T(2); Doxycycline; Bone microarchitecture; Micro-CT

1. Introduction

Second only to cardiovascular disease in producing long-term disability [1], osteoarthritis (OA) is a chronic degenerative disease in which the salient feature is the progressive loss of articular cartilage. Traditionally, OA has been diagnosed via radiographic examination, which relies on the assessment of late-stage indicators of disease such as joint space width and the presence of osteophytes for diagnosis [2,3]. Although effective, this approach is limited to assessing later stages of disease progression because soft tissues are poorly depicted using planar X-ray imaging techniques [4]. Moreover, in OA, the early stages of cartilage degeneration are often marked by the loss of specific biologic components of the cartilage matrix [5–8]. These cartilaginous changes affect the mechanical environment of the nearby bony plateaus, causing early-stage microstructural alterations in dynamic infrastructure, which could contribute to the progression of disease. Thus, considerable interest has focused on cartilage–bone interactions in OA, which may play a role in identifying future therapies.

Magnetic resonance imaging (MRI) has been used to assess cartilage morphology directly and has shown promise for the detection of soft-tissue changes [4,9–11]. In particular, $T_{1\rho}$ and T_2 relaxation times have proven to be valuable in the assessment of cartilage biochemistry, in particular hydration and collagen content and orientation [12,13]. T_2 tissue relaxation time has been found to be inversely correlated with both cartilage volume and thickness, and focal areas of increased T_2 have been found to correspond to cartilage lesions upon arthroscopic evaluation [12,14–16]. Lesions found in T_2-weighted images have also been correlated with degradations of the cartilage matrix (i.e., fibrillation, clefts [12,13]). $T_{1\rho}$ describes longitudinal relaxation in the rotating frame and has been associated with proteoglycan loss, which is thought to precede the development of symptomatic OA [10,17,18]. Thus, a unique and temporally dependent set of relative changes in $T_{1\rho}$ and T_2 values may reflect an osteoarthritic “footprint.” A biphasic increase and subsequent decrease in $T_{1\rho}$ and T_2 values likely track with disease progression, which is earmarked by initial inflammation and swelling followed by a balancing effect of proteoglycan and collagen loss with dehydration of the tissue, which would likely continue beyond the 12-week course of this study [5,8–11,13,18].

NIH-PA Author Manuscript

NIH-PA Author Manuscript

NIH-PA Author Manuscript

Assessment of bone quality in OA using MRI [11,13,18–20] and quantitative micro-computed tomography (μCT) of bone [21–23] has also revealed much information about ultra-structural bone density parameters and microarchitecture [24].

Although the disruptive and degradative events accompanying the advent of disease progression in OA are known [1,3–5], the mechanisms and order in which these events occur are still an active area of research [25–29]. Preclinical studies designed to address this need employ several animal models which exhibit disease phenotypes similar to those observed in humans [30–36].

To develop a framework for investigation in an animal model, we have characterized a method for observing longitudinal development of osteoarthritic disease as well as therapeutic efficacy in an in vivo rabbit anterior cruciate ligament (ACL) transection model of OA. To achieve this, we have longitudinally assessed the potential chondroprotective effects of doxycycline treatment in vivo using $T_{1\rho}$ and T_2 mapping techniques. We selected doxycycline as our treatment primarily because of the ease of administering therapy, as our goal was to establish the feasibility of longitudinal animal studies. The same techniques could be used to study other therapies for ACL transection models of OA such as *N*-acetyl glucosamine, hyaluronan and caspase [37–40].

Finally, we correlated these data with quantitative analyses of bone microstructure at 12 weeks in excised specimens to explore potential interactions between cartilage and bone in late-stage OA.

2. Methods

2.1. Experiment design

Twelve adult female New Zealand White rabbits, mean age 16 weeks (start weight 2.96±0.1 kg), underwent bilateral knee surgery. On the left, a medial arthrotomy was performed, and the ACL was transected (ACLX); on the right, only a medial arthrotomy was performed, but the intraarticular capsule was left intact (sham). Animals were anesthetized with an intramuscular injection of ketamine and xylazine, and wounds were covered with a local antibiotic ointment. Buprenorphine and nonsteroidal anti-inflammatory drugs were delivered to all animals for 2 days after surgery and as needed subsequently. Following surgery, the treatment group received 2.2 mg/kg doxycycline (MED4-VETS, Sandy, UT, USA) orally twice per day mixed with food for the duration of the study. Control animals received no treatment. Rabbits were imaged longitudinally at three time points up to 12 weeks (end weight 4.03±0.2 kg). Special MR-safe equipment was employed for anesthesia and monitoring. Furthermore, frequent medical checks during scans and recovery ensured that no rabbits were lost during this study. Total time required to scan each rabbit was 90 min. Rabbits tolerated the imaging protocol well and experienced no complications from anesthesia. Rabbits were euthanized by intraperitoneal overdose injection of sodium pentobarbital (>260 mg/kg) with subsequent bilateral thoracotomy. All animal experimentation was in accordance with institutional guidelines.

2.2. MR imaging and image processing

In vivo MRI data were acquired 3, 6 and 12 weeks postsurgery on a 3-T GE Excite Signa (General Electric, Fairfield, CT, USA) system using a quadrature transmit/receive knee coil. The protocol included three sequences: a sagittal three-dimensional (3D) water excitation high-resolution spoiled gradient-recalled (SPGR) imaging [repetition time (TR)/echo time (TE)=15/6.7 ms, flip angle=12, field of view (FOV)=12 cm, matrix=512×256, slice thickness=1 mm, bandwidth (BW)=31.25 kHz, number of excitation=1]; a sagittal 3D $T_{1\rho}$-weighted imaging sequence developed previously in our lab (TR/TE=9.3/3.7 ms; FOV=12

NIH-PA Author Manuscript

NIH-PA Author Manuscript

NIH-PA Author Manuscript

cm, matrix= 256×128, slice thickness=1 mm, BW=31.25 kHz, views per segment (VPS)=64, time of recovery (T_{rec})=1.5 s, time of spin-lock (TSL)=0, 10, 40, 80 ms, frequency of spin-lock (F_{SL})=500 Hz) and a T_2 quantification sequence (TE=4.1, 14.5, 25, 45.9 ms; all other parameters were the same as the $T_{1\rho}$ sequence) based on T_2 preparation pulses containing an Malcolm Levitt's composite-pulse decoupling sequence (MLEV) train of nonselective composite $90_x180_y90_x$ refocusing pulses.

Postprocessing of MR images to generate relaxation time maps was performed as described previously [11]. In brief, cartilage was segmented semiautomatically using SPGR images into lateral femoral condyle (LFC), medial femoral condyle (MFC), lateral tibia (LT) and medial tibia (MT) compartments. Following segmentation, a line was generated to artificially separate each region of the cartilage into medial and lateral compartments. The $T_{1\rho}$ map was reconstructed by fitting the image intensity pixel-by-pixel using a Levenberg–Marquardt monoexponential fitting algorithm developed in-house. $T_{1\rho}$-weighted images were rigidly registered to high-resolution SPGR images acquired in the same exam using the VTK CISG Registration Toolkit. The transformation matrix was applied to the reconstructed $T_{1\rho}$ map. The segmentation was corrected manually to avoid synovial fluid or other surrounding tissue. Three-dimensional cartilage contours were generated and overlaid on the registered $T_{1\rho}$ map. The T_2 map was reconstructed similarly using T_2-weighted images with the shortest TE.

2.3. μCT imaging and image processing

High-resolution, densitometric images for six animals were acquired using a commercial μCT system (μCT-40, Scanco Medical AG, Brüttisellen, Switzerland). This device consists of a microfocus X-ray source that produces a narrow-angle cone-beam incident upon a 2048×64-element CCD detector at 70 kV source potential and 117 μA current. Projection images spanning 1000 angles were collected over 180° with each projection sampled for 200 ms with two repetitions. The projections were then reconstructed across a 2048×2048 matrix spanning a 36.9-mm FOV, resulting in an isotropic nominal resolution of 18 μm. Each knee was imaged starting 9 mm proximal from the proximal extent of the distal femoral metaphyseal compartment and extending 9 mm distal to the distal extent of the proximal tibial metaphyseal compartment. The reconstructed linear attenuation values were calibrated against a phantom composed of five cylinders of known hydroxyapatite concentrations (0–800 mg HA/cm^3). This calibration served as the basis for equating reconstructed linear attenuation values to mineral density [41].

In the epiphysis, semiautomatic contours were generated in the coronal plane to define the volume of interest. Specifically, these contours identified the endosteal boundary to compartmentalize cancellous and cortical bone regions. Tibial and femoral epiphyses were analyzed independently, as were the medial and lateral compartments of each joint plateau. For each compartment, the image was smoothed with a constrained 3D Gaussian filter using different σ values for cortical and trabecular compartments (cortical: σ=1.2 kernel=5×5×5; trabecular: σ=1.0 kernel=3×3×3). This was done as the more compact cortex is often subject to greater noise and artifactual texture due to beam hardening and scatter effects, requiring more Gaussian smoothing. To avoid losing fine detail, less smoothing was applied to segment the trabecular voxels, which are smoother due to more partial signal contribution from the high surface area interface with marrow. We then applied an adaptive iterative threshold algorithm to segment the mineralized bone and marrow phases [42]. In the cancellous compartment, bone volume fraction (BV/TV) was determined by simple voxel counting of the bone and background phases. Mean trabecular dimensions [trabecular thickness (Tb.Th), number (Tb.N) and spacing (Tb.Sp)] and their distributions [Tb.Th.SD, Tb.(1/N).SD and Tb.Sp.SD] were calculated directly using a model-independent sphere filling technique [43]. Degree of anisotropy (DA) was calculated as the ratio of major and

NIH-PA Author Manuscript

NIH-PA Author Manuscript

NIH-PA Author Manuscript

minor principal components of the mean intercept length (MIL) ellipsoid. In the cortical compartment, cortical thickness (Ct.Th) was determined using direct 3D methods. The apparent and tissue mineral densities of the trabecular (Tb.BMD, Tb.TMD) and cortical (Ct.BMD, Ct.TMD) compartments were calculated as the mean calibrated grayscale values. The TMD parameters were calculated from all mineralized voxels excluding two layers of surface voxels with partial-volume contributions from marrow signal.

2.4. Statistical analysis

Mean values from each of three image slices for $T_{1\rho}$ and T_2 were calculated and averaged for each animal. The relaxation values for ACL-transected animals were normalized to the compiled average of all doxycycline-treated or untreated sham-operated animals, and results were analyzed using one-way temporal analysis of variance (ANOVA) and two-way ANOVA with repeated measures on one factor to assess intergroup variability over time and across surgery and treatment groups. Statistical significance was determined for a calculated P value of <.05 with a total of n=6 at each time point for each surgery–treatment combination.

Analysis of μCT data was facilitated by normalizing each parameter for each image set in either the femur or tibia by dividing by the average of that parameter across all animals (n=3 per group). Statistical significance for each metric was determined by a Student's t test with a P value of <.05.

Correlations between MRI and μCT data were determined by pairing each ACL-transected leg with its contralateral internal control and determining the difference in $T_{1\rho}$, T_2 and bone-densitometric parameters between the two legs for each animal (n=6). Pearson correlations were then calculated between $T_{1\rho}$ or T_2 values and each μCT parameter, grouping each femur and tibia compartment separately, as well as correlating doxycycline-treated animals and untreated animals separately. Statistical significance was determined for a calculated P value of <.05.

3. Results

3.1. In vivo MRI studies

Representative morphological images with $T_{1\rho}$ and T_2 map overlays are shown in Fig. 1. As illustrated in the image, the ACL-transected knee shows high $T_{1\rho}$ values in the weight-bearing region of the femoral condyle (red areas). In contrast, the sham-operated knee shows lower $T_{1\rho}$ values in the corresponding region (blue areas). Similarly, a representative T_2 map overlay is shown in Fig. 1. As seen in the image, the T_2 data also show increased values in the femoral condyle of the ACL-transected knee (yellow areas on weight-bearing portion of condyle). The sham-operated knee, in contrast, shows lower T_2 values in the weight-bearing region of the femoral condyle (blue areas on corresponding portion).

Fig. 2 shows sample ex vivo 3-D μCT images used for evaluation and analysis of the bony features of the femur and tibia compartments. These images were segmented, contoured and divided along the midline to define the regions of each compartment for processing.

Average sham-normalized $T_{1\rho}$ values of both ACL-transected groups at each time point are shown in Table 1A (n=6 for each treatment group at each time point). Absolute averages of each measurement for each group across the entire joint are shown in Table 2 for alternative perspective and reference. P values for the comparison between composite sham-operated and ACL-transected groups in each compartment at each time point are listed adjacent to the tables, while longitudinal P values are listed with each compartment in both groups. This analysis also showed that the only statistically significant relative difference in $T_{1\rho}$ values at

NIH-PA Author Manuscript

NIH-PA Author Manuscript

NIH-PA Author Manuscript

all time points between ACL-transected doxycycline-treated and untreated animals occurred in the LFC at 3 weeks (*P*=.01, data not shown). Furthermore, there was a statistically significant difference in average $T_{1\rho}$ values between sham-operated and ACL-transected animals at 3 weeks in the MFC, LT and MT (*P*=.0002, *P*=.03 and *P*=.01, respectively) and in the LFC at 12 weeks (*P*=.001), consistent with the representative image shown in Fig. 1.

Examining the data longitudinally, this initial elevation of $T_{1\rho}$ values of both treated and untreated MFCs 3 weeks after ACL transection decreased in relation to sham groups (which showed stable values during the entire 12-week course of the study, regardless of treatment type, *P*=.07 to .96, data not shown) by 12 weeks. The changes in $T_{1\rho}$ values of the MFC over time in the ACL-transected knees were found to be statistically significant in both doxycycline-treated and untreated groups (*P*=.04 and *P*=.0002, respectively). This pattern was mirrored in the doxycycline-treated LFC, LT and MT (*P*=.0002, *P*=.0005 and *P*=.008, respectively).

Table 1B lists sham-normalized T_2 values at each time point, as above. Only the LFC and MFC showed statistically significant differences between doxycycline-treated and untreated animals at the 3-week time point (*P*=.02 and *P*=.03, respectively; data not shown). The MFC demonstrated distinctions between ACL-transected and sham-operated knees at the 3- and 6-week time points (*P*<.0001 and *P*=.02, respectively), but there were no such distinctions observed in the LFC. Both tibia compartments show statistical significance when comparing sham-operated and ACL-transected groups only at all time points except for 12 weeks in the MT (LT: *P*=.03, <.0001 and .003; MT: *P*=.0002 and .04).

Examining the longitudinal T_2 relationships, values for the LFC and MFC show an initial elevation soon after ACL transection, particularly in doxycycline-treated knees. This elevation dropped significantly toward sham-operated values in the MFC for both treatment groups after 12 weeks (*P*=.02 and *P*=.004, respectively). Sham-operated knees remained stable during the course of study, regardless of treatment type (*P*=.1 to .96, data not shown). The LT also demonstrated a statistically significant change in T_2 values for untreated ACL-transected knees (*P*=.02), but this sequence differed in that values peaked at 6 weeks. Trends in the LFC and MT were similar to those seen in the MFC, but were not statistically significant (Table 1B).

3.2. μCT studies

Data collected from amputated rabbit legs using μCT imaging at 12 weeks, shown in Fig. 3, also demonstrate several statistically significant differences between ACL-transected and sham-operated knees. Table 3 lists absolute values and internal group variation for measured μCT parameters across the entire plateau of both the tibia and femur for reference (*n*=6). Among only untreated animals (*n*=3), there is a statistically significant decrease in BV/TV (*P*=.01), Ct.Th (*P*=.004) and Tb.BMD (*P*=.02) in the LFC of ACL-transected knees as compared to sham-operated knees. The MFC demonstrated a statistically significant decrease in DA (*P*=.03) in the ACL-transected animals compared to sham-operated rabbits. When only the doxycycline-treated rabbits are examined (*n*=3), these statistically significant differences disappear bilaterally. Notably, however, no significant differences in bone quality were found between doxycycline-treated and untreated animals in either femoral compartment of ACL-transected and sham-operated knees when considered individually.

In the tibia at 12 weeks, no statistically significant differences were found in bone densitometry between ACL-transected and sham-operated groups in the lateral compartment. In the medial compartment of untreated animals, however, statistically significant decreases in BV/TV (*P*=.001), Tb.BMD (*P*=.003), Tb.TMD (*P*=.01) and DA

NIH-PA Author Manuscript

NIH-PA Author Manuscript

NIH-PA Author Manuscript

(P=.04) are seen, and again, these mostly disappear when examining only doxycycline-treated animals.

3.3. MRI and μCT study correlations

Pearson correlation coefficients for the differences between single-rabbit ACL-transected and sham-operated knees in μCT parameters and $T_{1\rho}$ and T_2 relaxation at 12 weeks in the tibia and femur, with and without doxycycline, are summarized in Table 4 (n=6, three from each treatment group). Only statistically significant correlations are shown. Due to a technical challenge, the sham-operated tibia of one of the doxycycline-treated animals was not able to be processed for bone densitometry and was excluded.

4. Discussion

We performed longitudinal, in vivo $T_{1\rho}$ and T_2 MRI imaging in New Zealand White rabbits and examined the ability to longitudinally follow cartilaginous changes induced by ACL transection. Furthermore, after sacrifice, we performed μCT imaging to assess bony changes in this model at this late stage of OA. The data acquired for this in vivo study demonstrated general elevations of $T_{1\rho}$ and T_2 relaxation times in the tibia and femur of ACL-transected knees as compared to sham-operated knees at all time points, which is consistent with the findings seen previously in Lozano et al. [35]. Since elevations of $T_{1\rho}$ and T_2 values are associated with proteoglycan loss, collagen loss and hydration changes, the data suggest cartilage matrix destruction with biochemical disruption of the extracellular matrix.

Over time, however, $T_{1\rho}$ and T_2 relaxation times in the ACL-transected knees appeared to normalize to levels seen in sham-operated knees. This may be due to the rapid progression of cartilage loss and joint damage with subsequent loss of hydration, which has been observed in late-stage OA in previous studies, attributed to the loss of proteoglycans [44,45]. Dissection of ACL-transected joints after the 12-week MRI clearly revealed signs of severe OA, including synovial thickening and large osteophytes. This is consistent with a recent μCT study by Batiste et al. [21,22] demonstrating significant increases in osteophyte volume at 12 weeks after ACL transection in rabbits. The cartilage in the ACL-transected knee was likely desiccated, losing large amounts of extracellular matrix and water content, due to the loss of proteoglycans [44,45]. In the MFC, this could be a result of progressive water loss after initial swelling due to matrix disruption and proteoglycan loss from mechanical load changes in the injured joint, while in the lateral compartments, cartilage compression and direct mechanical injury led to dehydration and damage over time [46,47]. This damage-induced early-stage cartilage swelling and subsequent proteoglycan and cellular loss which leads to more the advanced cartilaginous derangements of late-stage OA have been studied previously [48,49]. By using our longitudinal, in vivo methodology, we may be able to better monitor therapeutic efficacy and molecular-level changes that begin during this initial phase.

The MFC only demonstrated statistically significant differences between the two surgery groups at the 3-week time point for $T_{1\rho}$ and the 3- and 6-week time points for T_2. This is likely due to elevations in the values caused by cartilage swelling and initial increase in matrix component synthesis with subsequent proteoglycan loss and concomitant water loss [46,47] resulting in a relative normalization of the relaxation times by 12 weeks. The MT also demonstrated universal elevations of $T_{1\rho}$ and T_2 in transected groups, suggesting that altered loading mechanics in the injured knees apply increased stress and compression forces to the tibial plateau, leading to cartilage damage [46].

The LFC did not display similar increased relaxation times in ACL-transected animals. This may reflect a more direct injury mechanism in the LFC due to ACL transection that results

NIH-PA Author Manuscript

NIH-PA Author Manuscript

NIH-PA Author Manuscript

in loss of cartilage volume as compared to the medial compartment where cartilage damage is secondary to altered knee-loading dynamics and subsequent loss of hydration and collagen [44–47]. The LT, on the other hand, more closely mirrors the response seen in the MT, with significant elevations across most time points. This could represent a downstream compensatory effect across the entire tibial plateau as forces on the knee joint are distributed more uniformly across the joint [46,47].

No statistically significant difference in cartilage quality, as measured by mean $T_{1\rho}$ and T_2 times, was seen between doxycycline-treated animals and untreated animals in the LT or MT. We speculate that, as a matrix metalloproteinase (MMP) inhibitor, doxycycline may not be as effective at slowing injury in the tibia where damage occurs through dynamic loading shifts that lead to matrix disruption [44]. In the femoral compartments, however, there was a statistically significant $T_{1\rho}$ relaxation time difference between untreated and doxycycline-treated animals at 3 weeks in the LFC and, for T_2, at 3 weeks in both the LFC and MFC. In this case, doxycycline's MMP inhibitory activity may help to mitigate proteoglycan breakdown and cartilage volume loss resulting from ACL injury. It is interesting to note that doxycycline administration causes a statistically significant change in $T_{1\rho}$ over time in all compartments, suggesting that, despite evidence of clinical markers, the presence of doxycycline may contribute to cartilage quality over time. However, the limited number of animals combined with the fact that the same animal was imaged longitudinally, unlike the temporally sacrificed animals seen in Lozano et al. [35], may result in patterns that are not fully consistent with those observed previously.

Although the randomized clinical trial led by Brandt et al. [26] suggests that doxycycline treatment should demonstrate reduced cartilage loss across the joint, the observed change was very small and across many animals, not likely to be detectable in our small-animal model with only 12 animals. Perhaps by increasing the number of animals, we could observe a similar universal effect by averaging out individual variability. In addition, it is also possible that the rapid progression of cartilage degeneration in these rabbits fails to provide enough time for doxycycline to effect much change. Even in previous canine studies of doxycycline prophylaxis in ACL-transected knees, doxycycline failed to prevent the rapid development of osteophytes [29]. Doxycycline may be more effective in early OA when the balance between MMP action and cartilage formation is only slightly skewed toward increased MMP activity, as seen by the early effects observed in the LFC and MFC.

Examining the data longitudinally demonstrates that sham-operated groups show stable relaxation times throughout the 12-week course of the study, regardless of doxycycline administration. As such, the changes observed in the ACL-transected cases are not likely to be a result of surgical access to the synovial compartment.

It is known that cartilage changes that occur in OA result in significant effects on bone health, leading to the clinical symptoms seen in advanced disease. By studying bone microarchitecture at 12 weeks, we are able to begin to elucidate bony changes and bone–cartilage interactions that occur in the ACL-transected model at a relatively late stage of OA. The trends we observed in this study are similar to what has been observed previously in ex vivo correlative studies and highlight the promise of this system as an in vivo longitudinal technique [4,21,22]. Although it might be expected that increased bone loading due to cartilage breakdown in OA would result in a mechanoreactive increase in bone metrics, this factor may be confounded by the change in the rabbit joint dynamics after injury [46,47]. Furthermore, our rabbits served as internal controls, and this favoring of the sham-operated leg could lead to both a decrease in bone density on the ACL-transected side and an opposing increase on the sham-operated leg.

NIH-PA Author Manuscript

NIH-PA Author Manuscript

NIH-PA Author Manuscript

Interestingly, however, the statistically significant differences between ACL-transected and sham-operated cases disappear in all compartments when doxycycline-treated animals are examined independently. Although these relationships are difficult to explore with few animals, we speculate that this suggests that the MMP inhibitory activity of doxycycline within the degenerating joints serves to improve cartilage health and thereby mitigates late-stage bony changes caused by injury-motivated joint unloading.

Considering both μCT and MRI data collected at 12 weeks begins to illuminate the relationship between cartilage and bone changes. This study does have several limitations, as it is difficult to infer any strong correlations from relatively few animals combined with the limited resolution of in vivo MRI scanning. However, some patterns can be studied from these relations, highlighting density loss and increased trabeculation in ACL-transected joints and the possible mitigation of these interactions with the introduction of doxycycline. However, this study was only able to assess bone quality at 12 weeks. As such, only potential late-stage associations, rather than predictive indicators, can be drawn from these correlations. Future experiments could collect μCT information throughout the progression of the disease, which may help to further identify correlations between localized changes in bone microarchitecture and $T_{1\rho}$ and T_2 maps of the overlying cartilage. In turn, this will help to elucidate bone–cartilage interactions in the development of OA and to identify future therapies that could effectively treat these targets.

In this study, $T_{1\rho}$ and T_2 were sensitive to early changes in cartilage induced by ACL transection. It may be useful to consider larger animal models for future studies. These animals do not develop cartilage degeneration as quickly as rabbits and may be a better model for early OA. However, in vivo imaging of large animals poses additional challenges: increased time commitment, cost and scan times. In addition, adjusting the protocol from having internal controls of the contralateral leg to using independent animal controls may be more effective for making quantitative comparisons over time. In addition, although the joint capsule was not compromised in sham-operated animals, future studies may obtain MRI scans at baseline before surgery to help assess the potential inflammatory effects of incision. The value of exploration of bone–cartilage interactions in a post-traumatic OA model, the time course of changes and the impact of therapies thus warrants further study.

References

1. Kotran, R.; Kumar, V.; Collins, T. Robbins pathologic basis of disease. Philadelphia: WB Saunders Company; 1999.
2. Rogers J, Watt, Dieppe P. A comparison of the visual and radiographic detection of bony changes at the knee joint. BMJ. 1990; 300:367–368. [PubMed: 2106987]
3. Altman R, Fries J, Bloch D. Radiographic assessment of progression in osteoarthritis. Arthritis Rheum. 1987; 30:11. [PubMed: 3814192]
4. Chan WP, Lang P, Stevens MP, Sack K, Majumdar S, Stoller DW, et al. Osteoarthritis of the knee: comparison of radiography, CT, and MR imaging to assess extent and severity. Am J Roentgenol. 1991; 157(4):799–806. [PubMed: 1892040]
5. Dijkgraaf LC, de Bont LG, Boering G, Liem RS. The structure, biochemistry, and metabolism of osteoarthritic cartilage: a review of the literature. J Oral Maxillofac Surg. 1995; 53(10):1182–1192. [PubMed: 7562173]
6. Bashir A, Gray ML, Burstein D. Gd-DTPA2- as a measure of cartilage degradation. Mag Res Med. 1996; 36(5):665–673.
7. Bashir A, Gray ML, Boutin RD, Burstein D. Glycosaminoglycan in articular cartilage: in vivo assessment with delayed Gd DTPA 2-enhanced MR imaging. Radiology. 1997; 205(2):551–558. [PubMed: 9356644]

NIH-PA Author Manuscript NIH-PA Author Manuscript NIH-PA Author Manuscript

8. Akella SV, Regatte RR, Gougoutas AJ, Borthakur A, Shapiro EM, Kneeland JB, et al. Proteoglycan-induced changes in $T_{1\rho}$-relaxation of articular cartilage at 4T. Magn Reson Med. 2001; 46(3):419–423. [PubMed: 11550230]
9. Mlynarik V, Szomolanyi P, Toffanin R, Vittur F, Trattnig S. Transverse relaxation mechanisms in articular cartilage. J Magn Reson. 2004; 169(2):300–307. [PubMed: 15261626]
10. Toffanin R, Mlynarik V, Russo S, Szomolanyi P, Piras A, Vittur F. Proteoglycan depletion and magnetic resonance parameters of articular cartilage. Arch Biochem Biophys. 2001; 390(2):235–242. [PubMed: 11396926]
11. Li X, Ma CB, Link TM, Castillo DD, Blumenkrantz G, Lozano J, et al. In vivo $T_{1\rho}$ and T_2 mapping of articular cartilage in osteoarthritis of the knee using 3 T MRI. Osteoarthritis Cartilage. 2007; 15(7):789–797. [PubMed: 17307365]
12. Broderick L, Turner D, Renfrew D, Schnitzer T, Huff J, Harris C. Severity of articular cartilage abnormality in patients with osteoarthritis: evaluation with fast spin-echo MR vs arthroscopy. AJR. 1994; 162:99–103. [PubMed: 8273700]
13. Blumenkrantz G, Dunn TC, Lindsey C, Ries MD, Link TM, SL S, et al. Cartilage T_2 as a marker of progression of osteoarthritis. Proceedings of ACR, San Antonio, TX. 2004:234.
14. Menezes NM, Gray ML, Hartke JR, Burstein D. T_2 and $T_{1\rho}$ MRI in articular cartilage systems. Magn Reson Med. 2004; 51(3):503–509. [PubMed: 15004791]
15. Dardzinski BJ, Mosher TJ, Li S, Van Slyke MA, Smith MB. Spatial variation of T_2 in human articular cartilage. Radiology. 1997; 205(2):546–550. [PubMed: 9356643]
16. Mosher TJ, Smith H, Dardzinski BJ, Schmithorst VJ, Smith MB. MR imaging and T_2 mapping of femoral cartilage: in vivo determination of the magic angle effect. AJR Am J Roentgenol. 2001; 177(3):665–669. [PubMed: 11517068]
17. Regatte RR, Akella SV, Lonner JH, Kneeland JB, Reddy R. $T_{1\rho}$ relaxation mapping in human osteoarthritis (OA) cartilage: comparison of $T_{1\rho}$ with T_2. J Magn Reson Imaging. 2006; 23(4): 547–553. [PubMed: 16523468]
18. Eckstein F, Burstein D, Link TM. Quantitative MRI of cartilage and bone: degenerative changes in osteoarthritis. NMR in Biomedicine. 2006; 19:822–854. [PubMed: 17075958]
19. Beuf O, Ghosh S, Newitt DC, Link TM, Steinbach L, Ries M, et al. Magnetic resonance imaging of normal and osteoarthritic trabecular bone structure in the human knee. Arthritis Rheum. 2002; 46:385–393. [PubMed: 11840441]
20. Kapadia RD, Stroup GB, Badger AM, Koller B, Levin JM, Coatney RW, et al. Applications of micro-CT and MR microscopy to study preclinical models of osteoporosis and osteoarthritis. Technol Health Care. 1998; 6(5–6):361–372. [PubMed: 10100939]
21. Batiste DL, Kirkley A, Laverty S, Thain LMF, Spouge AR, Gati JS, et al. High-resolution MRI and micro-CT in an ex vivo rabbit anterior cruciate ligament transection model of osteoarthritis. Osteoarthritis Cartilage. 2004; 12(8):614–626. [PubMed: 15262241]
22. Batiste DL, Kirkley A, Laverty S, Thain LM, Spouge AR, Holdsworth DW. Ex vivo characterization of articular cartilage and bone lesions in a rabbit ACL transection model of osteoarthritis using MRI and micro-CT. Osteoarthritis Cartilage. 2004; 12(12):986–996. [PubMed: 15564066]
23. Bouchgua M, Alexander K, d'Anjou MA, Girard CA, Carmel EN, Beauchamp G, et al. Use of routine clinical multimodality imaging in a rabbit model of osteoarthritis — parts I and II. Osteoarthritis Cartilage. 2009; 17(2):188–204. [PubMed: 18760939]
24. Blumenkrantz G, Lindsey CT, Dunn TC, Jin H, Ries MD, Link TM, et al. A pilot, two-year longitudinal study of the interrelationship between trabecular bone and articular cartilage in the osteoarthritic knee. Osteoarthritis Cartilage. 2004; 12(12):997–1005. [PubMed: 15564067]
25. Brandt KD. Modification by oral doxycycline administration of articular cartilage breakdown in osteoarthritis. J Rheumatol Suppl. 1995; 43:149–151. [PubMed: 7752122]
26. Brandt KD, Mazzuca SA, Katz BP, Lane KA, Buckwalter KA, Yocum DE, et al. Effects of doxycycline on progression of osteoarthritis: results of a randomized, placebo-controlled, double-blind trial. Arthritis Rheum. 2005; 52(7):2015–2025. [PubMed: 15986343]

NIH-PA Author Manuscript NIH-PA Author Manuscript NIH-PA Author Manuscript

27. Dieppe PA, Cushnaghan J, Shepstone L. The Bristol 'OA500' Study: progression of osteoarthritis (OA) over 3 years and the relationship between clinical and radiographic changes at the knee joint. Osteoarthritis Cartilage. 1997; 5(2):87–97. [PubMed: 9135820]
28. Jones MD, Tran CW, Li G, Maksymowych WP, Zernicke RF, Doschak MR. In vivo microfocal computed tomography and micro-magnetic resonance imaging evaluation of antiresorptive and antiinflammatory drugs as preventive treatments of osteoarthritis in the rat. Arthritis Rheum. 2010; 62:2726–2735. [PubMed: 20533290]
29. Yu LP Jr, Smith GN Jr, Brandt KD, Myers SL, O'Connor BL, Brandt DA. Reduction of the severity of canine osteoarthritis by prophylactic treatment with oral doxycycline. Arthritis Rheum. 1992; 35(10):1150–1159. [PubMed: 1329773]
30. Laurent D, O'Byrne E, Wasvary J, Pellas TC. In vivo MRI of cartilage pathogenesis in surgical models of osteoarthritis. Skeletal Radiol. 2006; 35(8):555–564. [PubMed: 16639625]
31. Bolbos R, Benoit-Cattin H, Langlois JB, Chomel A, Chereul E, Odet C, et al. Knee cartilage thickness measurements using MRI: a 4(1/2)-month longitudinal study in the meniscectomized guinea pig model of OA. Osteoarthritis Cartilage. 2007; 15(6):656–665. [PubMed: 17303445]
32. Wang YX. In vivo magnetic resonance imaging of animal models of knee osteoarthritis. Lab Anim. 2008; 42(3):246–264. [PubMed: 18625580]
33. Boulocher C, Chereul E, Langlois JB, Armenean M, Duclos ME, Viguier E, et al. Non-invasive in vivo quantification of the medial tibial cartilage thickness progression in an osteoarthritis rabbit model with quantitative 3D high resolution micro-MRI. Osteoarthritis Cartilage. 2007; 15(12): 1378–1387. [PubMed: 17576081]
34. Laurent D, Wasvary J, O'Byrne E, Rudin M. In vivo qualitative assessments of articular cartilage in the rabbit knee with high-resolution MRI at 3T. Magn Reson Med. 2003; 50(3):541–549. [PubMed: 12939762]
35. Lozano J, Saadat E, Li X, Majumdar S, Ma CB. Magnetic resonance $T_{1\rho}$ imaging of osteoarthritis: a rabbit ACL transection model. Magn Reson Imaging. 2009; 27(5):611–616. [PubMed: 19056196]
36. Yoshioka M, Coutts RD, Amiel D, Hacker SA. Characterization of a model of osteoarthritis in the rabbit knee. Osteoarthritis Cartilage. 1996; 4(2):87–98. [PubMed: 8806111]
37. Shikhman AR, Amiel D, D'Lima D, Hwag SB, Hu C, Xu A, et al. Chondroprotective activity of *N*-acetylglucosamine in rabbits with experimental osteoarthritis. Ann Rheum Dis. 2005; 64:89–94. [PubMed: 15608304]
38. Yoshioka M, Shimizu C, Harwood FL, Coutts RD, Amiel D. The effects of hyaluronan during the development of osteoarthritis. Osteoarthritis Cartilage. 1997; 5:251–260. [PubMed: 9404470]
39. Tiraloche G, Girard C, Chouinard L, Sampalis J, Mouquin L, Ionescu M, et al. Effect of oral glucosamine on cartilage degradation in a rabbit model of osteoarthritis. Arthritis Rheum. 2005; 52:1118–1128. [PubMed: 15818693]
40. D'Lima D, Hermida J, Hashimoto S, Colwell C, Lotz M. Caspase inhibitors reduce severity of cartilage lesions in experimental osteoarthritis. Arthritis Rheum. 2006; 54(6):1814–1821. [PubMed: 16736522]
41. Burghardt AJ, Kazakia GJ, Laib A, Majumdar S. Quantitative assessment of bone tissue mineralization with polychromatic micro-computed tomography. Calcif Tissue Int. 2008; 83(2): 129–138. [PubMed: 18685797]
42. Ridler TW. Picture thresholding using an iterative selection method. IEEE Trans Syst Man Cybern SMC. 1978; 8:630–632.
43. Hildebrand T, Ruegsegger P. A new method for the model-independent assessment of thickness in three-dimensional images. J Microsc. 1997; 185:67–75.
44. Song Y, Greve JM, Carter DR, Giori NJ. Meniscectomy alters the dynamic deformational behavior and cumulative strain of tibial articular cartilage in knee joints subjected to cyclic loads. Osteoarthritis Cartilage. 2008; 16:1545–1554. [PubMed: 18514552]
45. Stolz M, Gottardi R, Raiteri R, Miot S, Martin I. Early detection of aging cartilage and osteoarthritis in mice and patient samples using atomic force microscopy. Nature Nanotechnology. 2009; 4:186–192.

NIH-PA Author Manuscript

NIH-PA Author Manuscript

NIH-PA Author Manuscript

46. Chaudhari AM, Briant PL, Bevill SL, Koo S, Andriacchi TP. Knee kinematics, cartilage morphology, and osteoarthritis after ACL injury. Med Sci Sports Exerc. 2008:215–222. [PubMed: 18202582]

47. Herzog W. Muscle and joint biomechanics in the osteoarthritic knee. Proceedings of ICBME, Singapore. 2008; 23:2151–2154.

48. Calvo E, Palacios I, Delgado E, Ruiz-Cabello J, Hernández P, Sánchez-Pernaute O, et al. High-resolution MRI detects cartilage swelling at early stages of experimental osteoarthritis. Osteoarthritis Cartilage. 2001; 9:463–472. [PubMed: 11467895]

49. Calvo E, Palacios I, Delgado E, Sánchez-Pernaute O, Largo R, Egido J, et al. Histopathological correlation of cartilage swelling detected by magnetic resonance imaging in early experimental osteoarthritis. Osteoarthritis Cartilage. 2004; 12:878–886. [PubMed: 15501403]

NIH-PA Author Manuscript

NIH-PA Author Manuscript

NIH-PA Author Manuscript

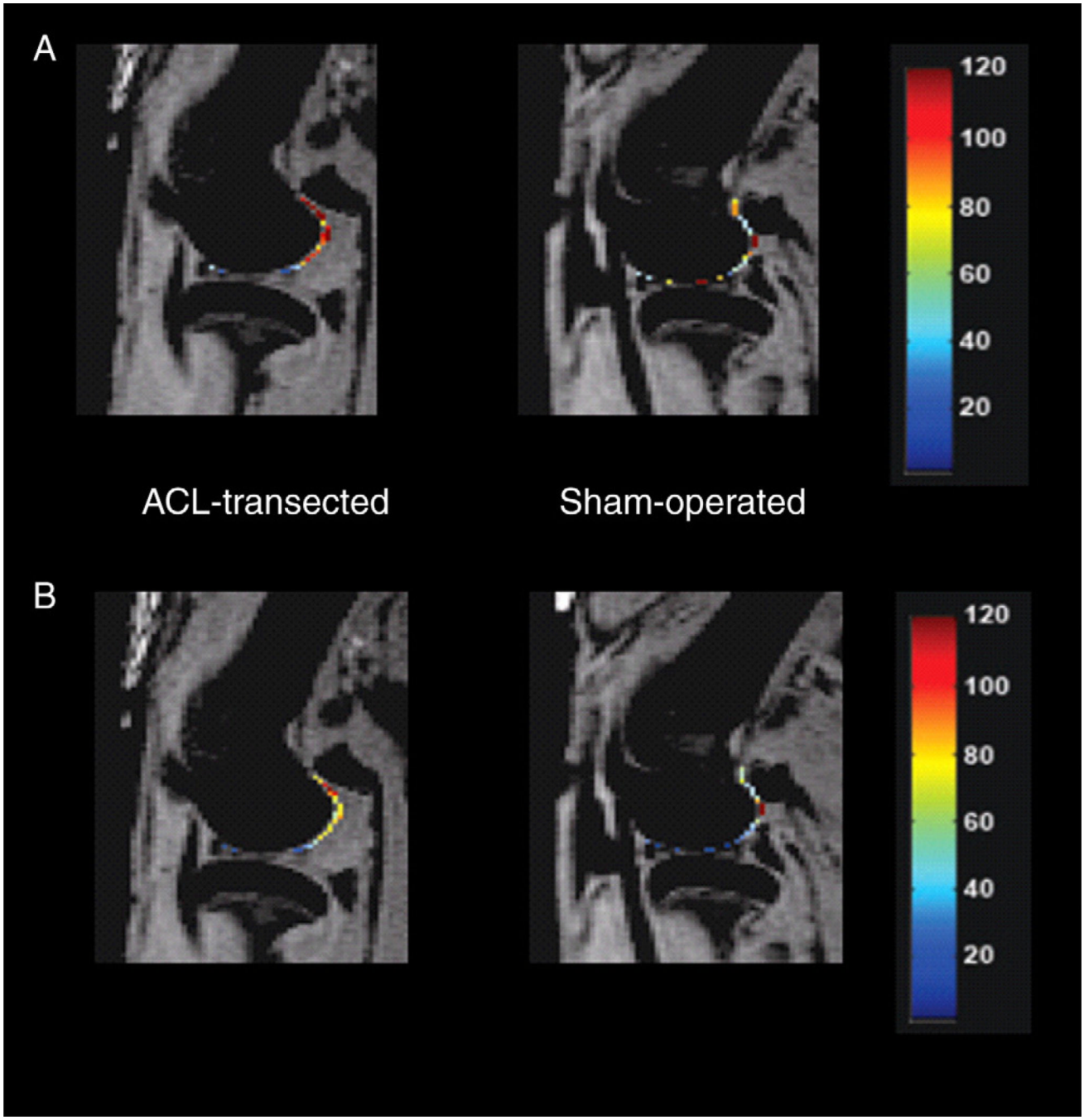

Fig. 1.

Representative $T_{1\rho}$ (A) and T_2 (B) maps of ACL-transected knee and the sham-operated knee in the same rabbit. Maps are overlaid on SPGR images. Images were acquired 3 weeks after surgery. An increase in both $T_{1\rho}$ and T_2 values on the weight-bearing portions of the femoral condyles in ACL-transected knees as compared to sham-operated knees highlights the typical changes in MRI signal found with osteoarthritic changes.

NIH-PA Author Manuscript

NIH-PA Author Manuscript

NIH-PA Author Manuscript

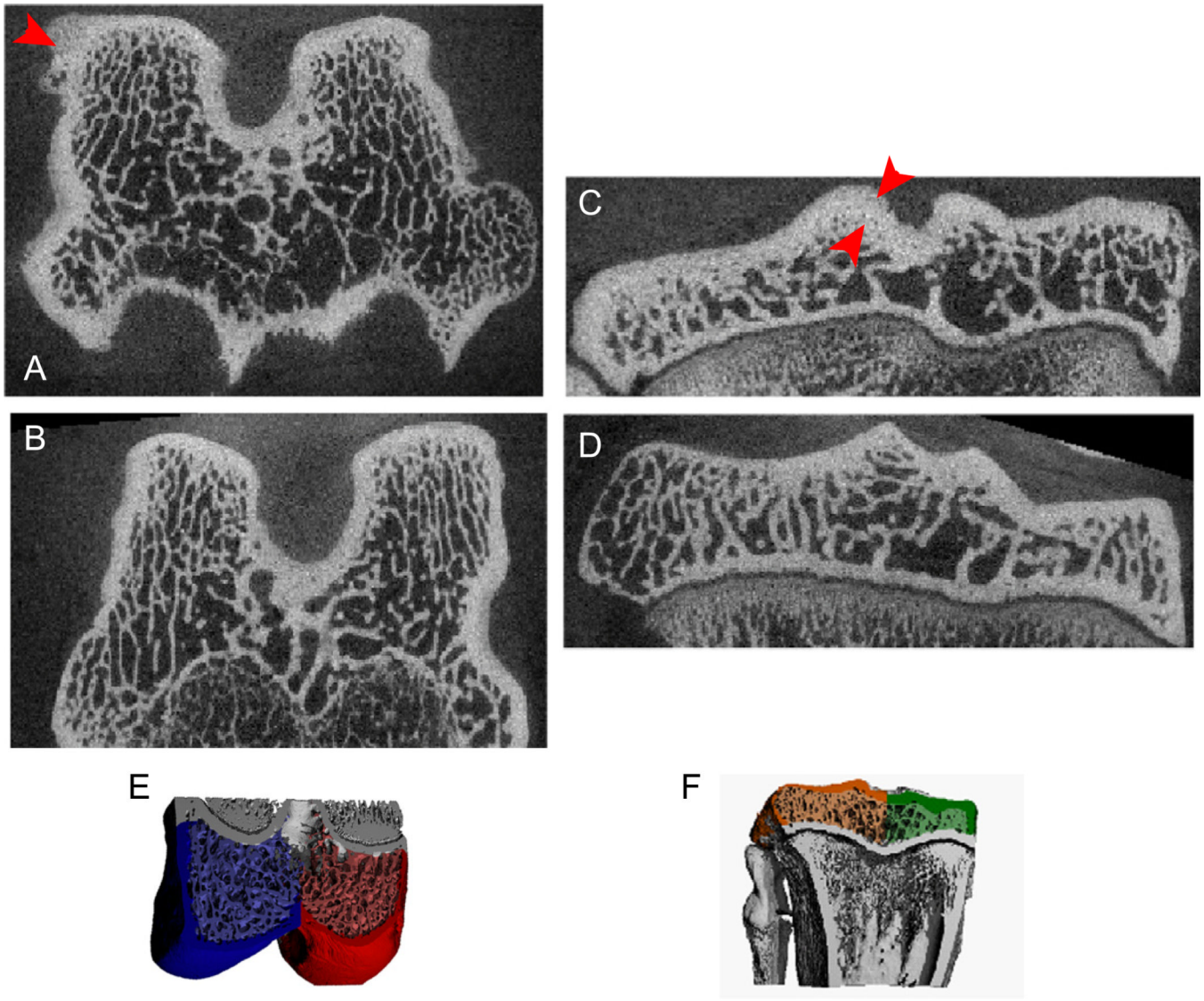

Fig. 2.

Example of images obtained using ex vivo μCT from the femur of an ACL-transected rabbit (A) and sham-operated rabbit (B), and the tibia of an ACL-transected rabbit (C) and sham-operated rabbit (D). Some macroscopic bony changes in ACL-transected rabbits can be appreciated, such as osteophytes and thickened, roughened cortical layers, as indicated by arrowheads. Sample imaged volumetric regions of interest of the femur (E) and tibia (F) with the medial compartments colored red and green and the lateral compartments shaded blue and orange are shown for illustration. (For interpretation of the references to color in this figure legend, the reader is referred to the web version of this article.)

NIH-PA Author Manuscript

NIH-PA Author Manuscript

NIH-PA Author Manuscript

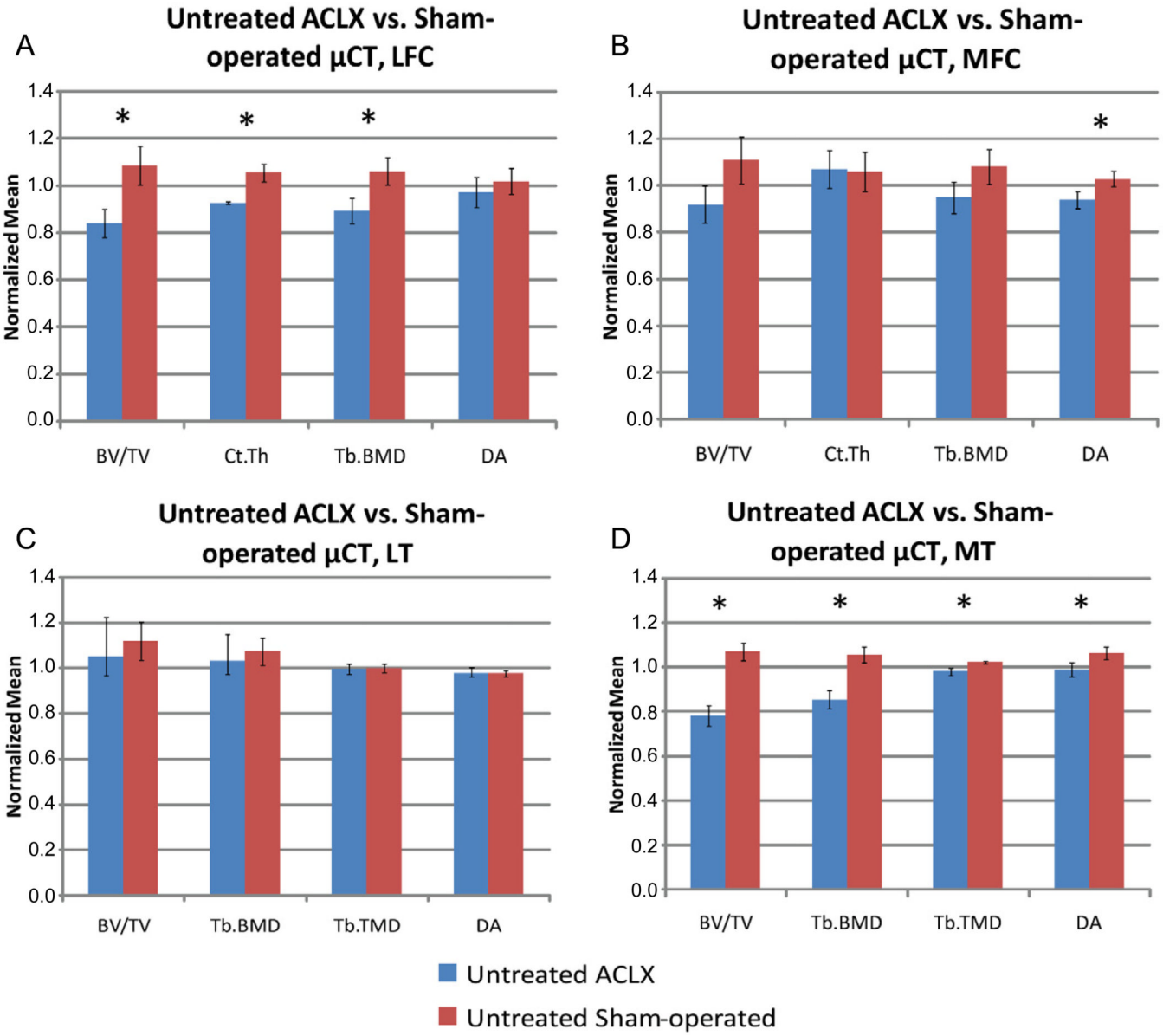

Fig. 3.

µCT results normalized to the average of each parameter across all compartments and groups. Only parameters that showed significant bone quality differences between ACL-transected and sham-operated knees in either the femur or tibia are shown for the LFC (A), MFC (B), LT (C) and MT (D) of untreated animals. Data represent three untreated rabbits from a group of six in which half were treated with doxycycline. Each animal had an ACL transection surgery (ACLX) on the left knee and a sham operation on the right knee. Error bars represent the 95% confidence interval of the normalized means. There is no significant difference in any of the bone quality values when considering only doxycycline-treated animals (data not shown). *P<.05 (specific values listed in Results).

NIH-PA Author Manuscript

NIH-PA Author Manuscript

NIH-PA Author Manuscript

Table 1

Relaxation time (ms) for each compartment normalized to relevant sham group

A

$T_{1\rho}$	ACLX Control (*n*=6)			ACLX Doxy (*n*=6)		
	3 Weeks	6 Weeks	12 Weeks	3 Weeks	6 Weeks	12 Weeks
LFC	0.92 +/- 0.06	0.86 +/- 0.12	0.79 +/- 0.04	1.15 +/- 0.07	1.02 +/- 0.08	0.87 +/- 0.05
	P=.09			***P*=.0002**		
LT	1.02 +/- 0.10	1.09 +/- 0.09	1.02 +/- 0.09	1.20 +/- 0.05	1.09 +/- 0.11	0.90 +/- 0.08
	P=.5			***P*=.0005**		
MFC	1.19 +/- 0.07	1.07 +/- 0.09	0.91 +/- 0.04	1.31 +/- 0.15	1.10 +/- 0.11	1.03 +/- 0.16
	***P*=.0002**			***P*=.04**		
MT	1.22 +/- 0.10	1.11 +/- 0.10	1.08 +/- 0.10	1.07 +/- 0.12	1.06 +/- 0.04	0.86 +/- 0.08
	P=.1			***P*=.008**		

	P-value (Surgery Group)		
	3 Weeks	6 Weeks	12 Weeks
LFC	0.4	0.3	**0.001**
LT	**0.03**	0.07	0.4
MFC	**0.0002**	0.07	0.6
MT	**0.01**	0.08	0.6

B

T_2	ACLX Control (*n*=6)			ACLX Doxy (*n*=6)		
	3 Weeks	6 Weeks	12 Weeks	3 Weeks	6 Weeks	12 Weeks
LFC	0.95 +/- 0.11	0.86 +/- 0.10	0.90 +/- 0.04	1.26 +/- 0.12	1.14 +/- 0.14	1.10 +/- 0.11
	P=.4			*P*=.2		
LT	1.10 +/- 0.16	1.53 +/- 0.19	1.29 +/- 0.18	1.31 +/- 0.21	1.38 +/- 0.24	1.22 +/- 0.19
	***P*=.02**			*P*=.6		
MFC	1.20 +/- 0.09	1.09 +/- 0.11	0.98 +/- 0.08	1.47 +/- 0.14	1.23 +/- 0.19	1.05 +/- 0.09
	***P*=.02**			***P*=.004**		
MT	1.24 +/- 0.09	1.15 +/- 0.12	1.10 +/- 0.10	1.22 +/- 0.08	1.18 +/- 0.12	1.16 +/- 0.16
	P=.2			*P*=.8		

	P-value (Surgery Group)		
	3 Weeks	6 Weeks	12 Weeks
LFC	0.09	0.97	0.98
LT	**0.03**	**<0.0001**	**0.003**
MFC	**<0.0001**	**0.02**	0.7
MT	**0.0002**	**0.04**	0.07

Longitudinal comparisons as determined by one-way ANOVA are represented by p-values in each compartment for each group of animals. In the adjacent sub-tables, p-values calculated using two-way ANOVA with repeated measures on one factor are also listed for the comparison of ACL-transection versus sham-operation across all treatment groups ("Surgery Group") to highlight the compartments and times at which ACL-transection resulted in significantly different measurements. Statisitcally significant p-values are highlighted in red. LFC = Lateral femoral condyle, LT = Lateral tibia, MFC = Medial femoral condyle, MT = Medial tibia.

Relaxation times measured by in vivo MRI and normalized to the average sham-operated values in each compartment across all time points (*n*=6 animals at each time point for untreated or doxycycline-treated, sham-operated animals ×3 time points=18) are shown with 95% confidence intervals.

NIH-PA Author Manuscript
NIH-PA Author Manuscript
NIH-PA Author Manuscript

Table 2

Absolute average relaxation time (ms) for all compartments per group

	A			
		3 Weeks	6 Weeks	12 Weeks
$T_{1\rho}$	Sham	54.6 +/− 3.2	53.6 +/− 3.4	54.2 +/− 3.2
	Sham + Doxycycline	53.0 +/− 3.0	54.0 +/− 3.6	58.6 +/− 4.2
	ACLX	59.0 +/− 2.4	54.9 +/− 2.7	50.8 +/− 2.1
	ACLX + Doxycycline	62.5 +/− 3.4	57.6 +/− 3.5	53.4 +/− 3.0
	B			
		3 Weeks	6 Weeks	12 Weeks
T_2	Sham	43.3 +/− 3.7	39.8 +/− 3.8	38.8 +/− 2.6
	Sham + Doxycycline	41.2 +/− 3.2	39.8 +/− 4.0	38.5 +/− 3.1
	ACLX	48.0 +/− 2.7	44.7 +/− 2.7	41.0 +/− 2.4
	ACLX + Doxycycline	54.2 +/− 4.4	48.7 +/− 4.7	43.5 +/− 3.0

Absolute average values of MR data across all animals and compartments in each surgery/treatment group, represented as sham-normalized quantities in Table 1A and B. Medial and lateral compartments of both the femur and tibia are grouped together. 95% Confidence intervals represent intragroup variability across all compartments. *n*=12 animals at all time points (six in each treatment group).

NIH-PA Author Manuscript NIH-PA Author Manuscript NIH-PA Author Manuscript

Table 3

Absolute average μCT values for entire joint plateau per group

		BV/TV	Ct.Th (mm)	Tb.BMD$_{(mgHA/cm^3)}$	Tb.TMD$_{(mgHA/cm^3)}$	DA
Tibia	Sham	0.465 +/− 0.027	——	459.414 +/− 18.970	767.419 +/− 13.885	1.349 +/− 0.070
	Sham + Doxycycline	0.453 +/− 0.046	——	454.236 +/− 31.171	775.261 +/− 3.074	1.354 +/− 0.048
	ACLX	0.389 +/− 0.079	——	406.893 +/− 53.614	749.642 +/− 15.129	1.300 +/− 0.036
	ACLX + Doxycycline	0.391 +/− 0.086	——	407.311 +/− 56.663	747.296 +/− 13.922	1.324 +/− 0.048
Femur	Sham	0.398 +/− 0.028	0.551 +/− 0.048	437.824 +/− 22.748	——	1.623 +/− 0.047
	Sham + Doxycycline	0.388 +/− 0.029	0.559 +/− 0.031	430.479 +/− 24.228	——	1.612 +/− 0.064
	ACLX	0.321 +/− 0.050	0.489 +/− 0.059	372.358 +/− 42.277	——	1.550 +/− 0.058
	ACLX + Doxycycline	0.311 +/− 0.027	0.527 +/− 0.049	370.221 +/− 25.336	——	1.504 +/− 0.078

Absolute average values of μCT parameters of both the tibia and femur, represented as normalized quantities in Fig. 3. Medial and lateral compartments are grouped together. Intragroup variability is represented by standard deviations. *n*=3 for all groups except in the sham+doxycycline group where *n*=2.

NIH-PA Author Manuscript NIH-PA Author Manuscript NIH-PA Author Manuscript

Table 4

Pearson correlations between μCT values and relaxation times

		BV/TV	Conn-Dens.	Tb.N	Tb.Th	Tb.Sp	Tb.BMD	Ct.TMD	DA	Tb.(1/N).SD	Ct.TMD
Untreated femur (n=3)	$T_{1\rho}$			0.86		−0.87				−0.90	0.85
	T_2		0.67	0.66		0.71		0.87	0.66		
Doxycycline-treated femur (n=3)	$T_{1\rho}$										
	T_2										
Untreated tibia (n=3)	$T_{1\rho}$										
	T_2	0.64		0.65	0.68		0.66				
Doxycycline-treated tibia (n=2)	$T_{1\rho}$		−0.76								
	T_2		−0.83						−0.80		

Pearson correlation coefficients for the differences between single-rabbit ACL-transected and sham-operated knees in μCT parameters and $T_{1\rho}$ and T_2 relaxation times at 12 weeks. Data were correlated for the six rabbits that had both MRI and μCT taken at 12 weeks (three treated with doxycycline, three untreated). Each group represents three animals, except in the case of doxycycline-treated tibia, where one animal's tibia data were excluded due to technical challenges which made these data inaccessible. Correlations all have P<.05. The threshold for significance at this level (P<.05) is ±0.622 when n=3 animals and ±0.729 when n=2. For clarity, only statistically significant correlations are shown.